Computer Simulation of Complexes of Dendrimers with Linear Polyelectrolytes

Sergey V. Lyulin,[†] Anatolij A. Darinskii,[†] and Alexey V. Lyulin*,[‡]

Institute of Macromolecular Compounds, Russian Academy of Sciences, Bolshoj pr. 31, 199004 St. Petersburg, Russia, and Group Polymer Physics, Eindhoven Polymer Laboratories and Dutch Polymer Institute, Technische Universiteit Eindhoven, P.O. Box 513, 5600 MB Eindhoven, The Netherlands

Received December 17, 2004; Revised Manuscript Received March 3, 2005

ABSTRACT: Brownian dynamics computer simulations have been carried out of complexes formed by charged dendrimers and oppositely charged linear polymer chains of different degree of polymerization N_{ch}. Bead−rod freely jointed models in the Debye−Hückel approximation without hydrodynamic interactions have been considered. Mean-square radii of gyration together with the radial density distribution functions have been calculated separately for a complex, a dendrimer, and a linear chain in a complex. The mean-square radius of gyration, the different monomer radial distribution functions, and the static structure factor for a dendrimer in a complex with long enough chains are very close to those for a single neutral dendrimer. The monomers of the linear chains with N_{ch} equal to the number of the dendrimer's terminal charged groups are located very close to these terminal groups. For longer chains the total number of the chain monomers adsorbed onto a dendrimer exceeds the number that is necessary for a dendrimer neutralization, and the overcharging phenomenon is observed. Comparison with predictions of the correlation theory has been carried out.

1. Introduction

The general trend in the modern development of biology, pharmaceutics, and medicine is closely related to the utilization of nanotechnology. One of the examples is gene therapy where drugs or genes are delivered into a cell in order to correct the genetic defects of damaged sites. DNA transport is closely related to this problem. The complexes of DNA with different compounds (e.g., nucleosomes, in which DNA is organized into a superhelix around a histone protein octamer,[1,2] DNA−cationic liposome complexes[3]) have been studied intensively. At present, viruses represent the most common agents used for gene delivery, but they are rather dangerous for an organism. At the same time polymers, which are the most well-known examples of the synthesized nanosized molecules, can be used as nanocontainers; however, their application is strongly restricted by the polydispersity.

Dendrimers represent novel polymer materials in which this disadvantage is corrected. The unique architecture and monodispersity allow the use of dendrimers as molecular cages for a direct transport of drugs and DNA. Two types of dendrimers are commercially available now: poly(amidoamine) dendrimers, or PAMAM (Aldrich Chemical Co. and Dendritech), and poly(propyleneimine) (PPI), or Astramol dendrimers (Aldrich and DSM Fine Chemicals).Their properties and potential applications have been intensively discussed.[4,5] Dendrimers have quite low toxicity in viva.[6] Zinselmeyer et al.[7] have recently shown that PPI dendrimers have in vitro low cytotoxicity, although an increase of toxicity at higher generations prevents their use as DNA delivery agents.

Usually complexes of dendrimers with other compounds in water are stabilized by electrostatic forces. In this case the host and guest molecules should contain charges of the opposite sign. There are some experimental data which throw light on the structure of such complexes. In particular, atomic force microscopy data[8] and titration combined with spectroscopy[9,10] indicate that DNA molecules wrap around charged dendrimer-like polymers. Nevertheless, the physical properties of charged dendrimers and their complexes with oppositely charged compounds (especially polyions) have been poorly investigated. Analytical consideration of such systems is restricted due to their extreme complexity. The first Monte Carlo (MC) simulation of complexes formed by dendrimers with charged terminal groups and oppositely charged linear chains has been performed recently by Welch and Muthukumar.[11] Main attention has been paid to the complexes of dendrimers with rather short linear chains; in this case the dendrimer charge is larger than that of a linear chain. The electrostatic interactions between charged groups were described by the screened Coulomb potential with the screening Debye radius determined by the salt concentration in the solution.

It is well-known that the formation of complexes of spherical macroions with low-molecular-weight ions or polyions is accompanied by so-called overcharging, where the overall charge of ions adsorbed on the macroion surface exceeds the initial charge of a macroion, so that the net charge of the complex changes sign. The overcharging effect has been intensively studied both experimentally and theoretically. The degree of the overcharging may be measured, for example, by the electrophoretic mobility[12] and light-scattering methods.[13] For the case of the dendrimer−polymer complex the linear polyelectrolyte is substantially adsorbed on the dendrimer surface. In this system the effect of the overcharging can be observed if the total

[†] Russian Academy of Sciences.
[‡] Technische Universiteit Eindhoven.
* To whom correspondence should be addressed. E-mail: a.v.lyulin@tue.nl.

10.1021/ma047403u CCC: $30.25
Published on Web 04/09/2005

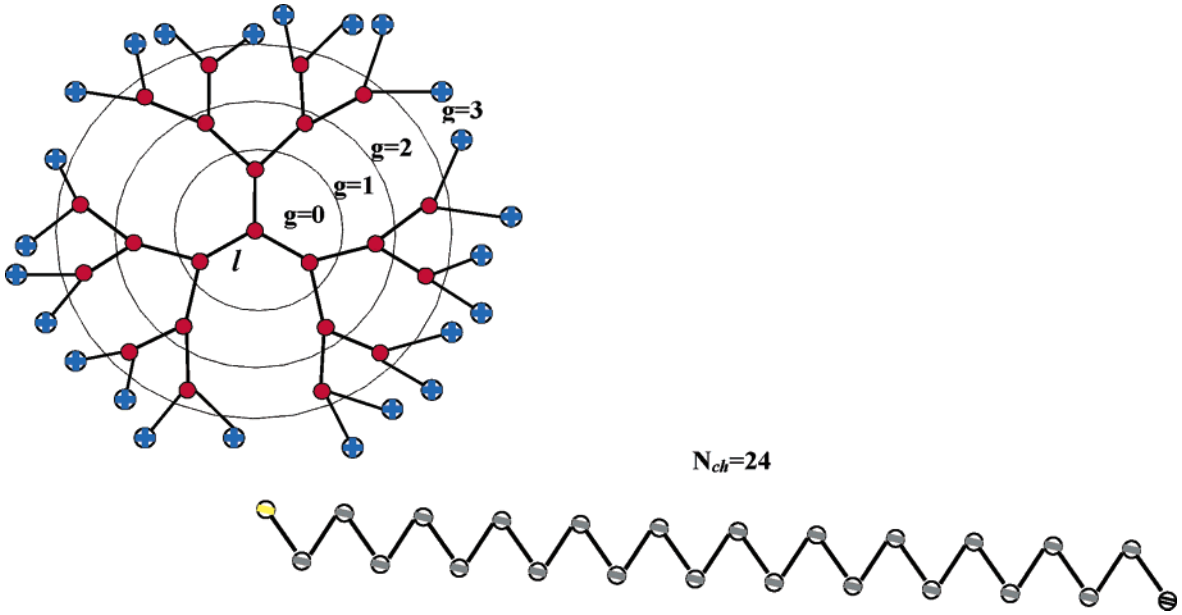

Figure 1. The freely jointed bead−rod model employed in this study: above example can be characterized as a $g = 3$ positively charged dendrimer with a $N_{ch} = 24$ negatively charged linear chain.

charge of a linear chain is larger than the dendrimer charge and will be manifested as an excess of a charge of adsorbed chain monomers over the dendrimer charge. Yager et al.[2] have shown that the negatively charged DNA molecule forms a complex winding around a positively charged liposome, and after enzymatic cutting of the DNA, the resulting nucleosome has a net negative charge. The effect of the overcharging attracts considerable attention because of its very special importance for gene delivery: it is known that usually the cell surface is charged negatively, and the complex, which includes drug or DNA, has to be charged positively in order to reach the cell. A number of simulation studies exist[14−18] where the overcharging of a hard-sphere macroion in a complex with oppositely charged linear chain has been observed. The mean-field analytical approach is usually used to describe the overcharging of an impenetrable macroion.[19−23] The overcharging degree of a complex formed by a charged hard sphere and an oppositely charged freely jointed chain has been studied in the MC simulation of Chodanowski and Stoll.[15] Their simulated results are in a good agreement with the theoretical predictions of Nguyen and Shklovskii.[20]

The overcharging effect is strongly influenced by solvent quality, radius of macroion, and flexibility of linear chain.[18,24] However, the systematic analytical and simulation studies of the inverse-charge phenomenon for objects which can be used as nanocontainers (i.e., for penetrable systems, including dendrimers) are absent. The first simulation efforts of complexes formed by nonspherical objects (proteins) and linear polyelectrolytes appeared only recently.[25]

The main goal of the present paper is to study the structure of a complex formed by a charged dendrimer and an oppositely charged linear chain by means of Brownian dynamics (BD) simulation. The main attention has been paid to sufficiently long linear chains, so the total charge of the chain in the considered complexes exceeds the dendrimer charge. The present study is limited to the simulation of complexes of charged linear chains and generation 1−4 dendrimers with terminal charged groups. The consideration of larger dendrimers and correspondingly larger linear chains needs much larger computer time. Nevertheless, even the present study allows one to obtain new and important conclusions about the structure of these complexes. We can add here that PAMAM dendrimers of such generations have been successfully used recently as drug delivery agents[26] and for DNA complexation.[10]

The remainder of the paper is organized as follows. In section 2 the model and simulation algorithm are described. In section 3 the statistical properties of a complex with linear chains of different length—the mean-square radius of gyration, the radial distribution function of monomers, the mass distribution, and the static structure factor—have been studied. The comparison with the properties of a single dendrimer has been made. The overcharging effect is described in section 4. Conclusions are summarized in section 5.

2. Model and Simulation Algorithm

2.1. Model of the Complex. We consider a bead−rod freely jointed model of a dendrimer[27−29] and of an oppositely charged linear chain (Figure 1). The dendrimer is represented as a system of beads connected by rigid bonds of length l. No valence- and torsion-angle potentials are taken into consideration. Dendrimers with a three-functional core and three-functional groups are studied. The $g = 0$ dendrimer consists of four beads including the core. Only dendrimers with rigid spacers consisting of one bond have been simulated. The total number of beads N in a generation-g dendrimer is calculated as

$$N = 3(2^{g+1} - 1) + 1 \qquad (1)$$

In the present simulation the case has been considered where all N_T terminal beads of a dendrimer are charged with the same charge $+e$. Such a situation is realized, for example, for PAMAM and other dendrimers in water solutions at neutral pH.[30,31] The linear chain is represented as a system of N_{ch} beads connected by rigid bonds of the same length l.

All the nonbonded beads in a dendrimer−linear chain complex interact via the modified Lennard-Jones po-

tential in which the attractive term is omitted

$$\tilde{U}_{\mathrm{LJ}}(r_{ij}) = 4\epsilon_{\mathrm{LJ}}\left[\left(\frac{\sigma}{r_{ij}}\right)^{12} - \left(\frac{\sigma}{r_{\mathrm{cut}}}\right)^{12}\right] \qquad r < r_{\mathrm{cut}}$$

$$\tilde{U}_{\mathrm{LJ}}(r_{ij}) = 0 \qquad r \geq r_{\mathrm{cut}} \tag{2}$$

where r_{ij} is the distance between ith and jth beads, ϵ_{LJ} and σ are the characteristic energy and length parameters, and r_{cut} is the cutoff distance, $r_{\mathrm{cut}} = 2.5\sigma$. This potential corresponds to the case of the athermal solvent. The values $\sigma = 0.8l$ and $\epsilon_{\mathrm{LJ}} = 0.3k_{\mathrm{b}}T$ have been taken from previous publications.[29,32]

Each bead of a linear chain is charged with the charge $-e$, and the total charge of the chain is equal to $-eN_{\mathrm{ch}}$. We suppose that the jth charged bead interacts with all other beads via the Debye−Hückel potential (electrostatic screened Coulomb potential)

$$\frac{U_j^{\mathrm{C}}}{k_{\mathrm{b}}T} = \lambda_{\mathrm{B}}\sum_i \frac{\exp(-kr_{ij})}{r_{ij}} \tag{3}$$

where r_{ij} is the distance between the charged beads i and j, and λ_{B} is the Bjerrum length describing the strength of the Coulomb interactions in a medium with dielectric constant $\tilde{\epsilon}$

$$\lambda_{\mathrm{B}} = \frac{e^2}{4\pi\tilde{\epsilon}k_{\mathrm{b}}T} \tag{4}$$

The value of λ_{B} in water at room temperature is 7.14 Å and is close to the segment length for a usual flexible polymer. Therefore, we put $\lambda_{\mathrm{B}} = l$ without much practical loss of generality.

The inverse Debye length k in eq 3 describes the screening of the electrostatic interactions due to the presence of counterions and salt in the real solution

$$k^2 = 4\pi\lambda_{\mathrm{B}}\sum_i z_i^2 c_i \tag{5}$$

Here c_i is the concentration of ith ion and z_i is its valence. The main effect of electrostatic interactions should be expected when the Debye length exceeds the size of the dendrimer. In the present study the value of $r_{\mathrm{D}} = k^{-1} = 8.96l$ is chosen (which corresponds to 2.2 mM aqueous salt concentration at 25 °C[11]), as was used by the authors previously for single charged dendrimers.[29,32] For the complexes where the dendrimer charge is compensated by the charge of the linear chain the counterions condensation should be small; it is hence not taken into account in this study.

The majority of the results have been obtained for complexes with $g = 3$ ($N = 46$, $N_{\mathrm{T}} = 24$) and $g = 4$ ($N = 94$, $N_{\mathrm{T}} = 48$) dendrimers in which the total linear-chain charge is equal to or exceeds the charge of the individual dendrimer, i.e., for $60 \geq N_{\mathrm{ch}} \geq 24$ (in complexes with $g = 3$ dendrimers) and for $90 \geq N_{\mathrm{ch}} \geq 48$ (in complexes with $g = 4$ dendrimers). Some results have been obtained for $g = 1$ and $g = 2$ dendrimers, only with the chain length $N_{\mathrm{ch}} = 48$, and for $g = 3$ dendrimers, with the short chain lengths $N_{\mathrm{ch}} = 5$ and $N_{\mathrm{ch}} = 15$.

2.2. Simulation Algorithm. In the present study the free-draining model has been chosen for the complexes. The main goal of the paper is the investigation of equilibrium properties of a dendrimer and a linear chain in these complexes. Neglecting the hydrodynamic interactions (HI) accelerates the calculations and does not influence the equilibrium properties. All beads of a system are characterized by the friction coefficient ζ. The finite-difference numerical scheme implemented here is based on the Ermak−McCammon equation[27−29] and was used for a simulation of a single charged dendrimer in the preceding publication.[29] The total force $\vec{F}_j^0$ acting on a bead j in the system is given by

$$\vec{F}_j^0 = -\sum_{k=1}^{N}\mu_k\left(\frac{\partial\nu_k}{\partial\vec{r}_j}\right)_r^0 - \partial\tilde{U}_{\mathrm{LJ}}/\partial\vec{r}_j^{\,0} - \partial U_j^{\mathrm{C}}/\partial\vec{r}_j^{\,0} \tag{6}$$

where $\nu_k = {}^1/_2(\vec{r}_{k+1} - \vec{r}_k)^2 - l^2 = 0$ is the equation for the kth rigid constraint, μ_k is the corresponding Lagrange multiplier, and $\vec{r}_j^{\,0}$ is the position vector for the jth bead before a time step Δt.

The SHAKE algorithm[33] with relative tolerance of 2×10^{-6} is used to maintain a fixed bond length. In the simulation dimensionless quantities are used in which the bond length l, the thermal energy $k_{\mathrm{b}}T$, and the translational friction coefficient $\zeta = 6\pi\eta_0 a$ (a is the hydrodynamic radius of a bead) were used as unit. It follows that time is expressed in units $\zeta/k_{\mathrm{b}}T$, the diffusion coefficient in units $k_{\mathrm{b}}T/6\pi\eta_0 a$, and the force in units $k_{\mathrm{b}}T/l$. The dimensionless integration step was chosen as $\Delta t = 10^{-4}$ in order to have the maximum displacement of a bead less than 10% of the bond length.

The initial configuration of a dendrimer is built using a procedure similar[27−29] to that proposed by Murat and Grest.[34] The core bead is put into the center of the coordinate system. Onto the core bead, along the X, Y, and Z axes, three monomers are attached, which constitute the generation $g = 0$ dendrimer. The next generation is built adding two monomers to each of the free ends of the $g = 0$ dendrimer. The distance between a newly added bead and all the previous beads is constrained to be larger than some distance $r_{\mathrm{min}} = 0.8\sigma$. Obviously, as g increases, it becomes increasingly difficult to fulfill the constraint of no overlap of beads. If a bead cannot be inserted after a set of 1000 trials, the whole dendrimer is discarded, and the process is started again with a new random-number seed.

To create the initial configuration of the chain, the maximum values of coordinates of all dendrimer beads x_{max}, y_{max}, and z_{max} have been calculated. The first bead of a linear chain has the coordinates $x_{\mathrm{max}} + 1$, y_{max}, z_{max}. Then a linear polymer chain has been initially created in a planar extended configuration with fixed valence angles $\Theta = 90°$ (Figure 1).

The initial configuration of each complex is equilibrated for 6−11 runs of 2×10^6 steps each, and then seven production runs of 2×10^6 time steps are performed. During each run the instantaneous values of the squared radius of gyration R_{g}^2 are calculated, for both the complexes and the individual chain and a dendrimer in it:

$$\langle R_{\mathrm{g}}^2\rangle = \frac{1}{N+1}\sum_{n=0}^{N}\langle(\vec{r}_n - \vec{r}_{\mathrm{C}})^2\rangle \tag{7}$$

Here $\vec{r}_{\mathrm{C}}$ is the radius vector of the corresponding center of mass, $\vec{r}_n$ is the radius vector of the nth bead, and brackets denote the averaging over all time steps during the run.

During the equilibration, the mean-square radius of gyration of a dendrimer remains almost unchanged, and

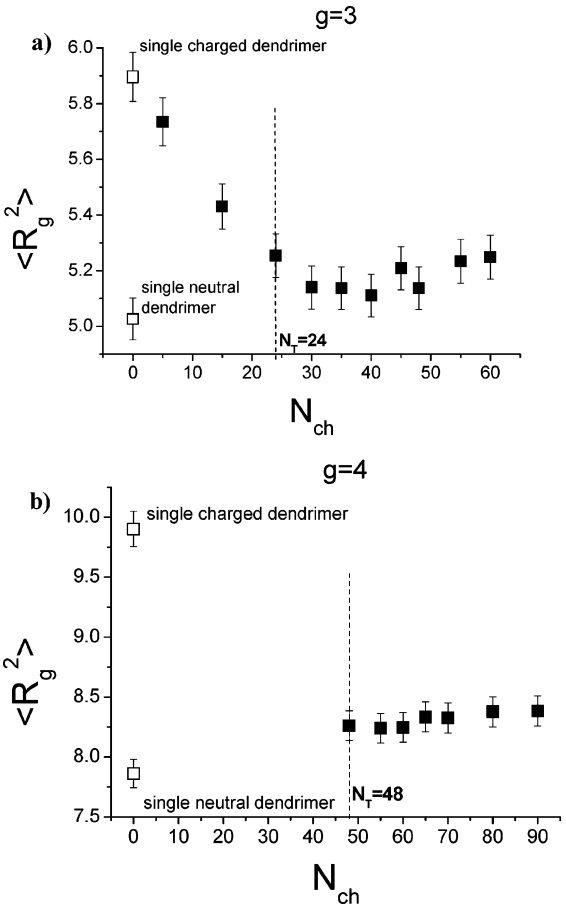

Figure 2. Mean-square radius of gyration of (a) $g = 3$ and (b) $g = 4$ dendrimer in a complex (filled symbols) with different chains, and of the individual dendrimers (open symbols). Case $N_{ch} = 0$ corresponds to a single (neutral and charged) dendrimer. N_T is the number of terminal groups in the dendrimer. Data for single charged dendrimers are also shown.

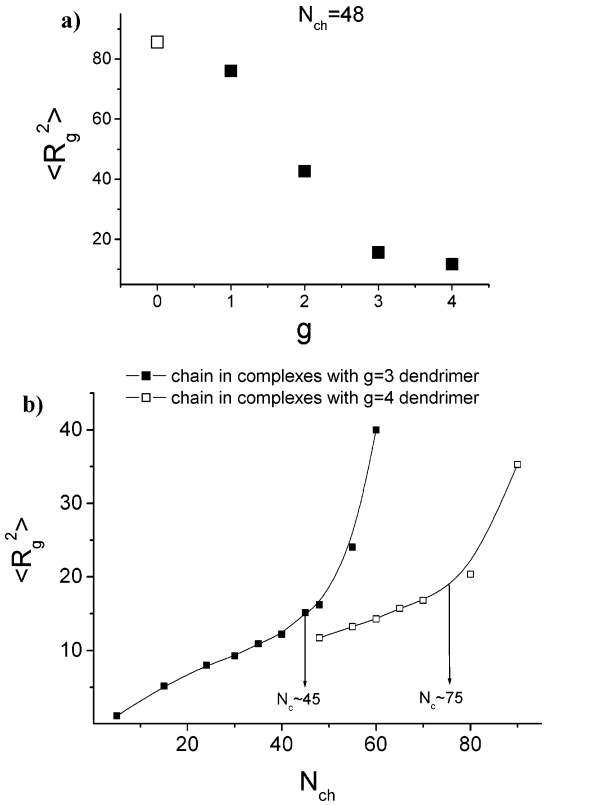

Figure 3. (a) Mean-square radius of gyration of a linear chain in a complex (filled squares) with dendrimers as a function of dendrimer generation g and mean-square radius of gyration of a single chain (open square). (b) Mean-square radius of gyration of a linear chain in a complex with $g = 3$ (filled squares) and $g = 4$ (open squares) dendrimers as a function of chain length. At $N_{ch} \geq N_c$ the overcharging takes place.

the length of the whole equilibration procedure is completely determined by the time of the linear-chain equilibration (about 500 steps for a complex of a $g = 4$ dendrimer and an $N_{ch} = 48$ chain).

3. Statistical Properties of the Complex

3.1. Mean-Square Radius of Gyration. We calculated the mean-square radius of gyration $\langle R_g^2 \rangle$ separately for a dendrimer and for a linear chain in a complex as well as for the complex as a whole. The dendrimer mean-square radius of gyration in a complex with chains of different length is shown in Figure 2 as a function of the chain length for both $g = 3$ and $g = 4$ dendrimers. For a $g = 3$ dendrimer and $N_{ch} < 24$ the length of these short chains is not enough to compensate the charge of a dendrimer. The value of the mean-square radius of gyration decreases with increase of the chain length, and saturation takes place when the number of beads in a chain, N_{ch}, is equal to the total number of the dendrimer terminal groups, N_T.

In the simulated complexes the density of charged beads is rather high. The presence of these charges leads to the strong screening of electrostatic interactions. Therefore, the size of a dendrimer in a complex is not changed with increasing the length of a linear chain above N_T. In Figure 2 $\langle R_g^2 \rangle$ for a dendrimer in a complex is compared with that for a single neutral and for a charged dendrimer[29] at the same value of the Debye screening length. Both for $g = 3$ and for $g = 4$ dendrimers $\langle R_g^2 \rangle$ for a dendrimer in a complex is very close to that for a single neutral dendrimer at $N_{ch} > N_T$. It means that the linear chain in a complex is adsorbed by the dendrimer. The degree of this adsorption will be discussed later in connection with the overcharging effect. We conclude here that the value of the mean-square radius of gyration for a dendrimer in a complex with long chains, $N_{ch} > N_T$, is closer to that for a neutral dendrimer and differs significantly from the mean-square radius of gyration of an individual charged dendrimer with the same value of the Debye length, $r_D = 8.96$.

The mean-square gyration radius of a linear chain decreases significantly (as compared to the individual chain) after the formation of a complex. Figure 3 shows this behavior for a $N_{ch} = 48$ chain which forms a complex with $g = 1-4$ dendrimers. Open squares correspond to the mean-square gyration radius of a single charged chain in the Debye−Hückel approximation with the same value of the Debye length r_D. The lowest value of the mean-square radius of gyration for a $N_{ch} = 48$ chain in all considered complexes corresponds to the case of the complexation with a $g = 4$ dendrimer, of which the charge is equal to the total charge of this chain. Figure 3b shows the chain mean-square radius of gyration $\langle R_g^2 \rangle$ in complexes with $g = 3$ and $g = 4$ dendrimers as a function of N_{ch}. Two different regimes are observed. First, $\langle R_g^2 \rangle$ slowly increases with increase of N_{ch} until some value of $N_c \sim 45$ and $N_c \sim 75$ in complexes with $g = 3$ and $g = 4$ dendrimers, respectively. In this adsorption regime up to $N_{ch} = N_c$ almost

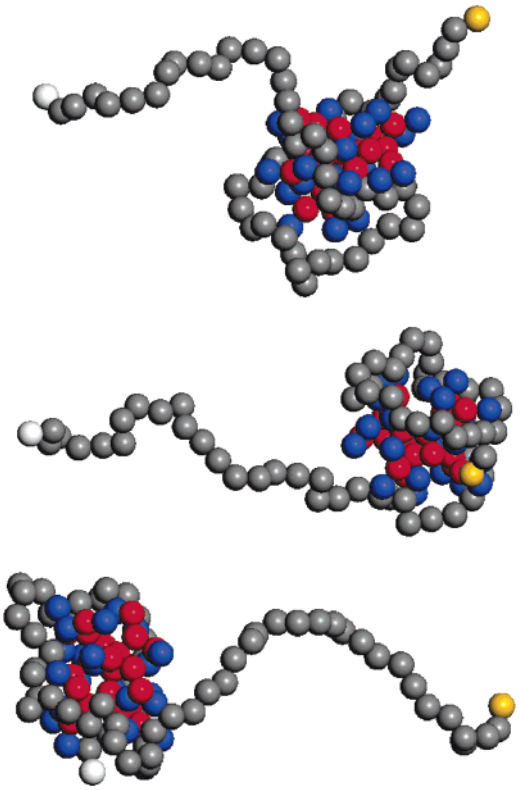

Figure 4. Typical snapshots of a complex formed by a $g = 3$ dendrimer and $N_{ch} = 60$ linear chain at three different times. Terminal groups of the dendrimer are colored in blue, and the internal monomers are colored in red. Chain beads are colored in gray. Different chain ends are colored in white and yellow.

all chain monomers are adsorbed onto a dendrimer, and only small tails or loops outside the dendrimer exist. With further increase of N_c longer tails appear, which in turn leads to a stronger increase of the chain mean-square radius of gyration in the second regime. Such values of N_c may correspond to overcharging in the considered complexes. This assumption will be further discussed in section 4.

When the total charge of a chain exceeds the total charge of a dendrimer, the chain in a complex is in a compact folded conformation with one or two tails; see the snapshots in Figure 4 for complexes formed by a $g = 3$ dendrimer and a $N_{ch} = 60$ linear chain. The snapshots show the migration of a dendrimer from one chain end to another similar to the findings of Welch and Muthukumar.[11] To characterize this motion, we intend to study the dynamical properties of the dendrimer−linear chain complex in our future investigations.

3.2. Radial Density Distribution. To study the location of different monomers in the complexes (the beads of a dendrimer in a complex and the beads of a linear chain in a complex), the radial density distribution function of beads, $\rho(r)$, is calculated as

$$\rho(r) = \frac{\langle n(r) \rangle}{V(r)} \tag{8}$$

where $\langle n(r) \rangle$ is the average number of beads in a spherical layer at a distance r from the corresponding center of mass and $V(r)$ is the volume of the layer.

In Figure 5a the radial density distribution functions of monomers of a $g = 4$ dendrimer in complexes with linear chains of different lengths are shown together

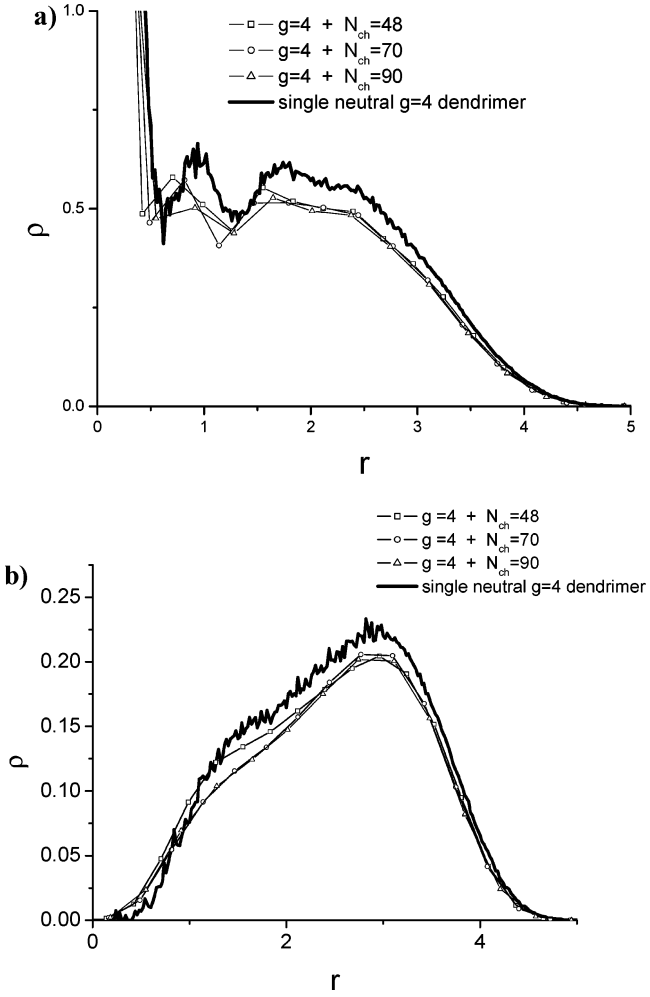

Figure 5. (a) Density distribution functions of monomers of a $g = 4$ dendrimer in complexes with different chains. (b) Density distribution functions of terminal groups of a $g = 4$ dendrimer in complexes with different chains. In all figures the density distribution functions of single neutral dendrimers are shown (bold solid lines).

with distribution functions for a single neutral dendrimer. The radial distribution functions for dendrimer monomers in complexes with different chains change weakly with the increase of the chain length and are close to those for a single neutral dendrimer. The same tendency is observed for terminal groups (Figure 5b) and for the groups belonging to the different generation shells of a given dendrimer (not shown). Thus, the distribution of the dendrimer monomers in the complexes with different chains is practically the same and close to that for a single neutral dendrimer. The same results are observed for a $g = 3$ dendrimer (not shown).

In Figure 6 the monomer radial distribution functions for monomers of complexes, dendrimer monomers in complexes, and chain monomers in complexes are shown.

We observe a rather high degree of a chain penetration inside the dendrimer. In Figure 6 the maximum in the distribution of the chain monomers is clearly located inside the corresponding dendrimer. The distribution of the linear-chain monomers inside the dendrimer is of special interest. In particular, the strong penetration of a chain into a dendrimer may complicate the chain release, which would make the use of the considered dendrimers as nanocarriers impossible.

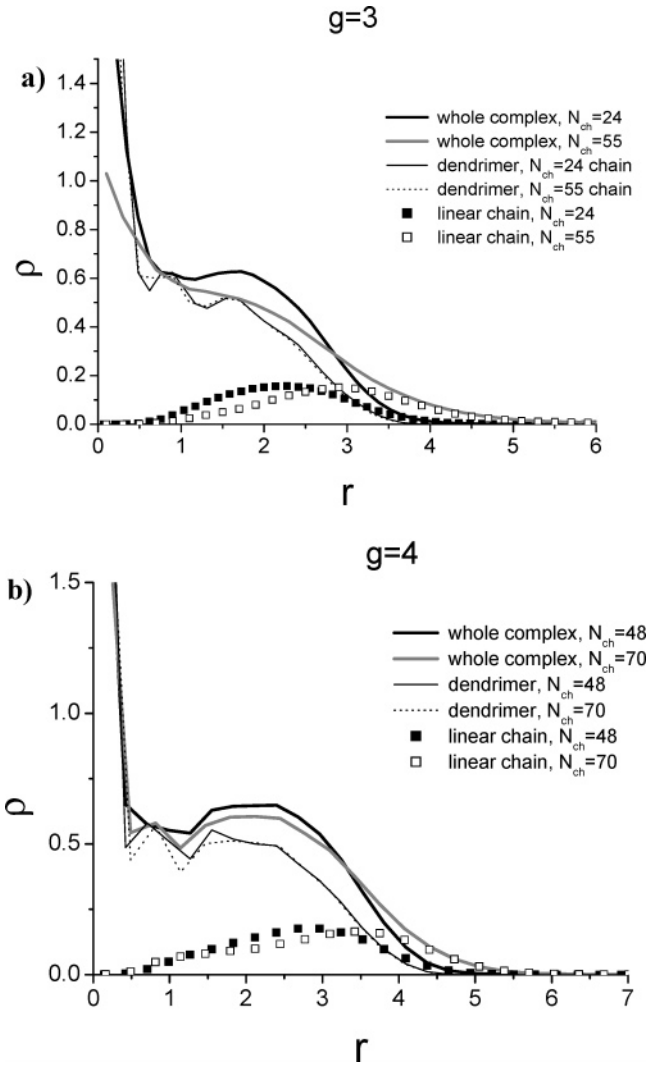

Figure 6. (a) Density distribution functions for monomers in complexes with a $g = 3$ dendrimer. (b) Density distribution functions for monomers in complexes for a $g = 4$ dendrimer.

To understand better the chain location inside a dendrimer, we compare the radial distribution functions of the chain monomers in complexes and those of the dendrimer terminal groups (Figure 7). It is clearly seen that the distribution of the dendrimer terminal groups in the complexes with different linear chains remains almost the same as for a single neutral dendrimer. Then, the distribution of the chain monomers with $N_{ch} = N_T$ ($N_{ch} = 24$ and $N_{ch} = 48$ in a complex with $g = 3$ and $g = 4$ dendrimers, respectively) is close to the distribution of the dendrimer terminal groups. It means that the chain monomers are located near the charged terminal groups of a dendrimer. With increase of the chain length, the maximum in the distribution of the chain monomers shifts to the exterior part of a dendrimer.

3.3. Mass Distribution. The integral characteristic of the monomers distribution in a complex is the mass distribution function $M(r)$ (the total number of monomers in a sphere with a center which coincides with the center of mass of a complex) shown in Figure 8. With increasing the distance r the value of mass increases as $M(r) \sim r^3$ for both $g = 3$ and $g = 4$ dendrimers, which corresponds to a dense sphere. For short chains ($N_{ch} \sim 24$ in a complex with a $g = 3$ dendrimer and $N_{ch} \sim 48$ in a complex with a $g = 4$ dendrimer) the saturation in

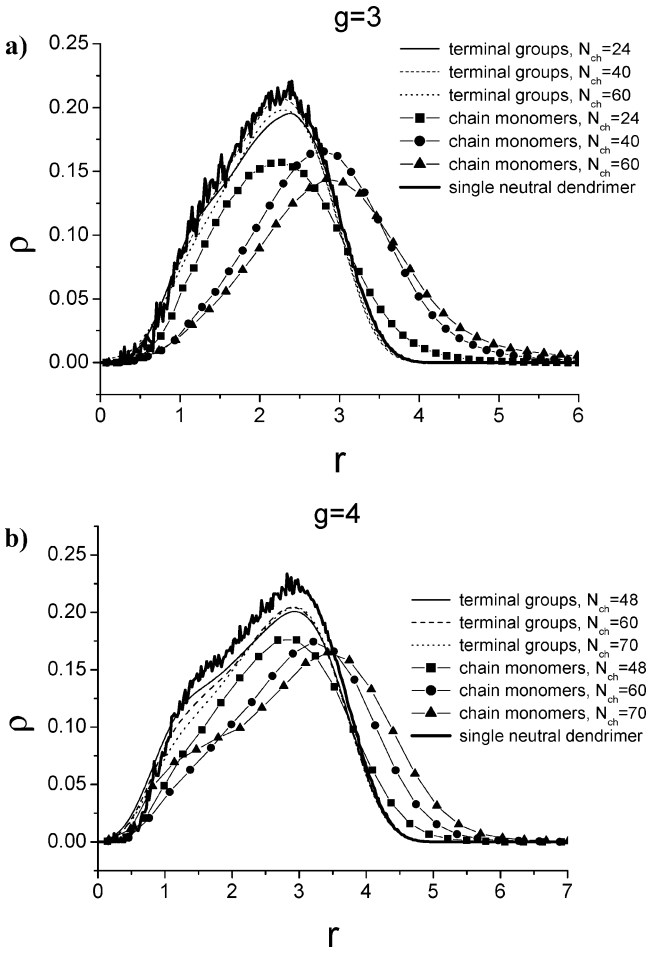

Figure 7. Density distribution functions of the terminal groups for a dendrimer in complexes and chain monomers in complexes for (a) $g = 3$ and (b) $g = 4$ dendrimers. The density distribution functions of the terminal groups of individual neutral dendrimers are also shown in both figures.

the r dependence of the mass distribution function $M(r)$ is observed at larger distances as compared to the single neutral dendrimer. Such a saturation at larger distances corresponds to the full chain adsorption onto a dendrimer. For longer chains ($N_{ch} > 45$ and $N_{ch} > 60$ for complexes with $g = 3$ and $g = 4$ dendrimers, respectively) the dependence $M(r) \sim r^3$ changes into a much weaker dependence, which corresponds to the tails still present in the complex. As shown in Figure 8 at large distance ($r \sim 8$) the value of M changes nonmonotonically with increase of the chain length N_{ch}. It may correspond to the nonmonotonic changing of the number of chain monomers adsorbed onto a dendrimer with increase of N_{ch}. We suppose that this effect is directly connected with the similar nonmonotonic behavior of the overcharging degree which will be discussed later.

3.4. Static Structure Factor. Experimentally the structure of a complex can be studied by small-angle neutron scattering (SANS). The scattered radiation intensity is proportional to the static structure factor

$$S(q) = \langle |\sum_{n=1}^{N} \sum_{m=1}^{N} e^{i\vec{q}\cdot(\vec{r}_n - \vec{r}_m)}|^2 \rangle \qquad (9)$$

which is measured directly in the present simulations. Here $\vec{q}$ is the scattered radiation vector, $q = |\vec{q}| = (4\pi/\lambda) \sin(\Omega/2)$, Ω is the scattering angle, λ is the

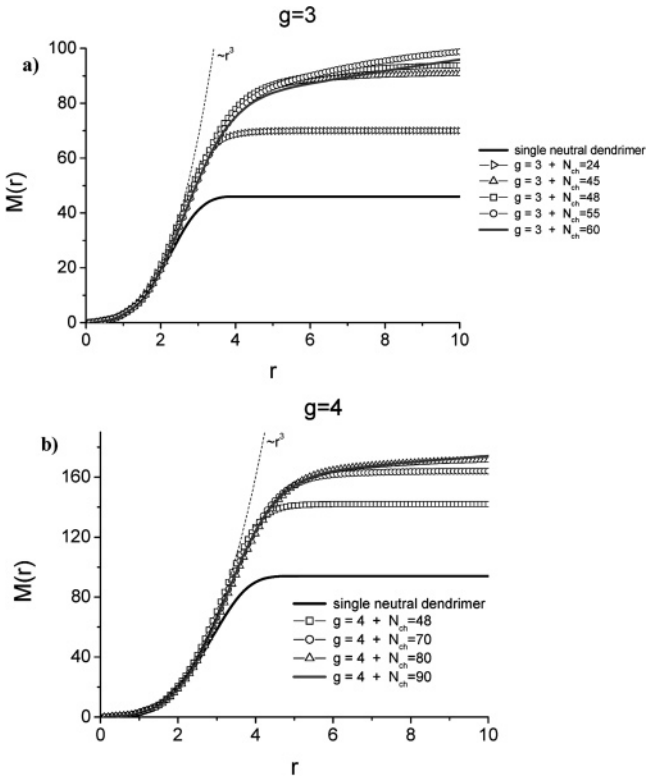

Figure 8. Mass distribution in complexes with (a) $g = 3$ and (b) $g = 4$ dendrimers.

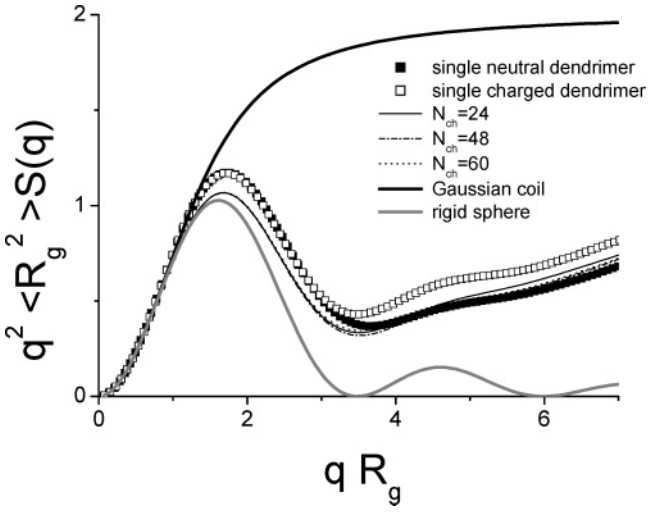

Figure 9. Kratky plot representation of the structure factor N_{ads} for a $g = 3$ dendrimer in a complex with different chains. Results for single neutral and single charged dendrimers with $r_D = 8.96$, Gaussian coil, and rigid sphere are shown as a reference.

wavelength, and $\vec{r}_n$ are the coordinates of the scattering centers. In Figure 9 the Kratky plot representation for a structure factor of a $g = 3$ dendrimer in complexes with different chains is shown. Such a structure factor can be measured experimentally for complexes with labeled dendrimers or linear chains. Qualitatively the same picture is observed for a $g = 4$ dendrimer.

The static structure factor of a dendrimer in a complex does not depend on the chain length and is close to that for a single neutral dendrimer (filled squares in Figure 9). The structure factor is closer to that for a rigid sphere (gray bold line in Figure 9) and differs significantly from that for a Gaussian coil (bold line in Figure 9).

4. Dendrimer Overcharging

We have already shown that a linear chain in complexes is significantly adsorbed onto a dendrimer. In this section we discuss the overcharging effect for the dendrimer in a complex.

For a hard sphere with the total charge placed in its center[2,12−23] the phenomenon of the charge inversion is well established and calculated in many simulation studies, and agreement with theoretical predictions has been obtained. The chain monomer is considered as adsorbed onto a sphere with radius R if the distance between the center of the bead and the center of a sphere does not exceed $R + l$, where l is the bond length.[15,16]

Correlation theory[20] predicts the following change of the structure of a complex as the chain length $N_{ch} = N_n$ increases starting from the chain length N_{ch} that is necessary for the neutralization of a sphere. At $N_{ch} \geq N_n$ the chain as a whole adsorbs onto a sphere until the value of N_{ch} reaches some critical value N_C. At this point the first-order phase transition takes place, and a chain tail is released. Upon increasing further the chain length the length of a tail increases. At the same time the length of the adsorbed chain decreases, finally achieving the saturation value N_∞ ($N_C > N_\infty > N_n$). Nguyen and Shklovskii[20] calculated the value of the chain length N_C at which the tail release occurs, the length of the chain tail in this critical point, and the saturation value N_∞ for adsorption degree. Calculated values strongly depend on the total charge of a sphere and weakly depend on it radius. Such analytical predictions of Nguyen and Shklovskii[20] for adsorption of a wormlike chain onto an oppositely charged hard sphere are in an excellent agreement with MC simulations of Chodanowski and Stoll[15,16] for adsorption of a linear chain onto an oppositely charged hard sphere. They considered the polymer chain as a succession of N freely jointed tangent spheres that interact via a hard-sphere potential to account for excluded-volume interactions, plus a screened Coulomb potential between pointlike charges. Each sphere is considered to be a physical monomer with a radius σ_m equal to 3.57 Å. The bond length l between the monomers is constant and equal to the Bjerrum length $\lambda_B = \lambda = 2\sigma_m = 7.14$ Å whereas the fraction of ionized monomers is set to 1. An impenetrable uniformly charged sphere with a radius σ_p is used to represent the charged colloidal particle. The ratio σ_p/σ_m is varied between 2 and 50.

Strictly speaking, for non-hard-spherical objects like dendrimers the criterion of chain adsorption is not defined. We suggest the following "local" criterion for calculation of the total number of the adsorbed chain monomers N_{ads} onto a dendrimer. The chain bead r_i is considered to be adsorbed onto a dendrimer if there exist another dendrimer bead r_j, such that $|r_i - r_j| < r_c$, where r_c is some parameter. To avoid the strong influence of the Lennard-Jones repulsion, the value of r_c was chosen to be equal to $r_c = 1 + \sigma = 1.8l$. The calculated value of N_{ads} is plotted in Figure 10 (filled circles).

Is it possible to use the old "spherical" criterion for adsorption, representing the dendrimer as a hard sphere or not? As shown by Nguyen and Shklovskii,[20] a wormlike chain with total charge equal to the charge of a sphere is completely adsorbed onto a sphere. The smallest value r_{ov} of the radius of a sphere representing the dendrimer at which the chain with $N_{ch} = N_T$ is completely adsorbed onto this sphere can be found:

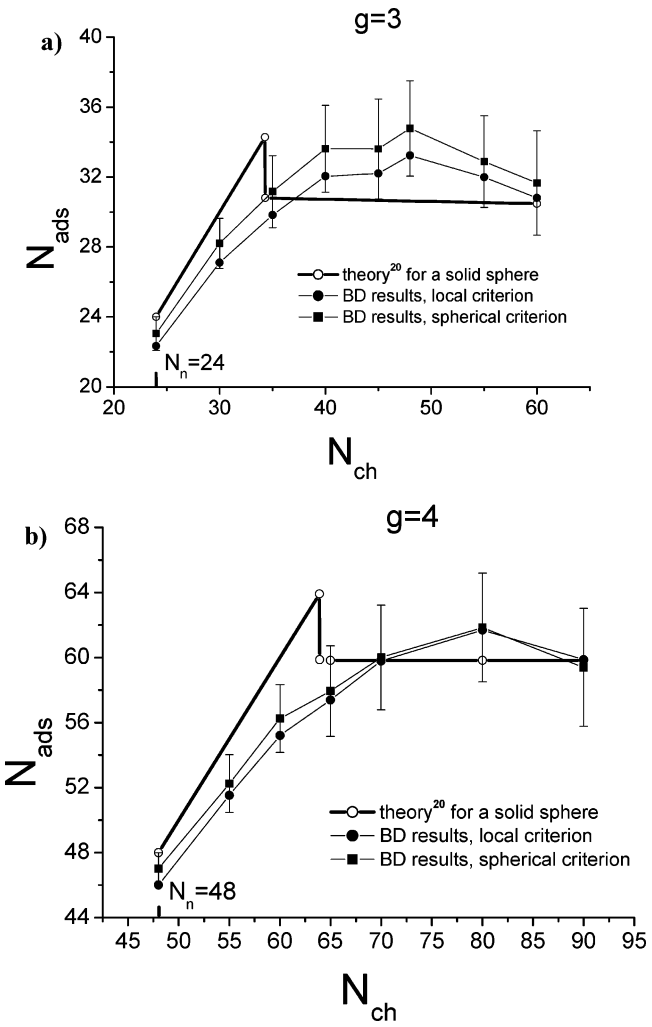

Figure 10. Dependence of the number of the adsorbed linear chain monomers N_{ads} on the chain length N_{ch} for complexes with (a) $g = 3$ and (b) $g = 4$ dendrimers. $N_n = N_T$ is the chain length which is necessary for the neutralization of a dendrimer.

$r_{ov} = 3.2$ and $r_{ov} = 4$ for $g = 3$ and $g = 4$ dendrimers, respectively. These radii exceed the corresponding dendrimer radius of gyration. We calculated N_{ads} for all considered complexes with $g = 3$ and $g = 4$ dendrimers, considering the dendrimer as a sphere with radius r_{ov} and using the "spherical" criterion for adsorption. The results obtained for the degree of the chain adsorption are also shown in Figure 10 (filled squares) together with the theoretical predictions of Nguyen and Shklovskii[20] for spheres with the same radius (bold lines with open circles). We can see that both ("local" and "spherical") determinations of the chain adsorption give approximately the same results; i.e., the overcharging does not depend on the criterion. At chain lengths $N_{ch} > N_T$ the total number of the chain monomers adsorbed onto a dendrimer exceeds the number that is necessary for the dendrimer neutralization; i.e., the overcharging phenomenon is observed.

The nonmonotonic behavior in the dependence N_{ads} (N_{ch}) is observed in agreement with the theoretical predictions,[20] but BD simulations show also some differences in the dependence N_{ads} (N_{ch}): (i) the onset of the decrease of N_{ads} with increasing N_{ch} is eroded; (ii) the chain length at which N_{ads} starts to decrease is shifted to larger values of N_{ch} as compared to the theoretical predictions. The onset of the decrease of N_{ads} starts from $N_{ch} \sim 50$ and $N_{ch} \sim 80$ for complexes with $g = 3$ and $g = 4$ dendrimers, respectively, in accordance with conclusions obtained earlier from the chain-length dependence of the mean-square radius of gyration of a chain in a complex (Figure 3b).

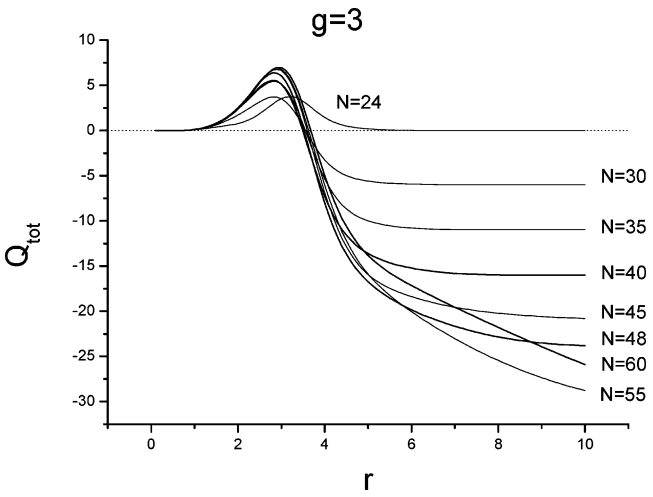

Figure 11. Total charge Q_{tot} inside the complex (linear chain with a $g = 3$ dendrimer) as a function of the distance from the center of mass of the complex.

In the present study a dendrimer with a charge distributed through the whole volume (and not only at a surface as in the case of the impenetrable sphere!) has been simulated. As was shown by the authors earlier,[29,32] the linear-chain monomers penetrate into the interior of a dendrimer since the dendrimer has sufficient empty volume inside. So, the main difference from the theoretical models considered earlier (see ref 20) is related to the penetrability of a dendrimer. It would be rather useful to consider analytically a system in which the impenetrable sphere is replaced by a charged spherical layer, where the charge is distributed through the whole volume and adsorbed linear-chain monomers have additional possibility for the localization near the opposite charges inside the layer.

The dependence of the number of the adsorbed chain monomers N_{ads} on the ionic strength represents a special interest. We plan to study this problem on a later stage, when the simulations of charged dendrimers with explicit counterions will be carried out.

The dependence of the total charge of the complex on the distance from its center of mass is shown in Figure 11. At small distances the total charge Q_{tot} is equal to zero—no charged chain segments or charged terminal groups can be found there. Then the value of charge Q_{tot} passes through the positive maximum at some distance which corresponds to the maximum in the distribution function of the terminal groups. Finally, the saturation takes place at some negative value of the charge which corresponds to the total ($N_T - N_{ch}$) charge of the complex. As for the dependence N_{ads} (N_{ch}), the nonmonotonic N_{ch} dependence of the distance r at which the total charge Q_{tot} is equal to zero has been observed (Figure 11).

5. Conclusions

Brownian dynamics computer simulations have been carried out of complexes formed by model charged dendrimers of generations $g = 3$ and $g = 4$ and the oppositely charged linear polymer chains of different degree of polymerization N_{ch}. Bead−rod freely jointed

models have been explored in the Debye−Hückel approximation and without hydrodynamic interactions. The statistical properties of a charged dendrimer in a complex with an oppositely charged linear chain (dendrimer mean-square radius of gyration, radial distribution of monomers, distribution of the dendrimer terminal groups, and structure factor) remain almost the same as for a single neutral dendrimer and differ significantly from that for an individual charged dendrimer with the same value of the Debye screening length. Starting from the chain length $N_{ch} > N_T$ (in this case all electrostatic interactions are almost screened), these statistical properties do not depend on the chain length.

At the same time, the radius of gyration of the linear chain is changed considerably and depends on the dendrimer generation number. The majority of the linear-chain monomers in the complexes are located near the dendrimer terminal groups that facilitate the chain release. Strong adsorption of the chain on a dendrimer exists for chain lengths exceeding the length $N_{ch} = N_T$ which is necessary for the neutralization of a dendrimer. The mean-square radius of gyration, radial density distribution function, mass distribution, and structure factor are all strongly influenced by this adsorption. The exact amount of adsorbed chain monomers can be obtained from the investigation of the overcharging effect. The criterion for calculation of the overcharging degree for penetrable objects like dendrimers is defined locally. The overcharging effect is observed for all simulated complexes. This effect is in a qualitative agreement with the predictions of the correlation theory for a hard-sphere model.[20] However, the onset of the phase transition (the tail appearance) is eroded and is shifted to the higher values of the chain length.

Acknowledgment. The authors are indebted to Prof. dr. M. A. J. Michels (Eindhoven University of Technology and Dutch Polymer Institute), Prof. T. Birshtein (Institute of Macromolecular Compounds, St. Petersburg), and Dr. A. Gurtovenko (Helsinki University of Technology) for many useful discussions. This work was carried out with the financial support of the Netherlands Organization for Scientific Research (NWO Grant 047.009.017), ESF programs SIMU and STIPOMAT, Russian Foundation for Basic Research (Grant 05-03-32450-à). S.V.L. is grateful to the Academy of Finland for the partial support of this work (Grant 211579).

References and Notes

(1) Luger, K.; Mäder, A. W.; Richmond, R. K.; Sargent, D. F.; Richmond, T. J. *Nature (London)* **1997**, *389*, 251−260.
(2) Yager, D.; McMurray, C. T.; van Holde, K. E. *Biochemistry* **1989**, *28*, 2271.
(3) Rädler, J. O.; Koltover, I.; Salditt, T.; Cyrus, R. Safinya, C. R. *Science* **1997**, *275*, 810−814.
(4) Liu, M. J.; Frechet, M. J. *Pharm. Sci. Technol. Today* **1999**, *2*, 393−401.
(5) Frechet, J. M. J.; Tomalia, D. A. *Dendrimers and Other Dendritric Polymers*; Wiley: New York, 2002.
(6) Roberts, J. C.; Bhalgat, M. K.; Zera, R. T. *J. Biomed. Mater. Res.* **1996**, *30*, 53−65.
(7) Zinselmeyer, B. H.; Mackay, S. P.; Schatzlein, A. G.; Uchegbu, I. F. *Pharm. Res.* **2002**, *19*, 960.
(8) Gössl, I.; Shu, L.; Schlüter, D.; Rabe, J. P. *J. Am. Chem. Soc.* **2002**, *124*, 6860−6865.
(9) Kabanov, V. A.; Zezin, A.Â.; Rogacheva, V. B.; Gulyaeva, Zh. G.; Zansochova, M. F.; Joosten, J. G. H.; Brackman, J. *Macromolecules* **1999**, *32*, 1904.
(10) Kabanov, V. A.; Sergeyev, V. G.; Pyshkina, O. A.; Zinchenko, A. A.; Zezin, A.Â.; Joosten, J. G. H.; Brackman, J.; Yoshikawa, K. *Macromolecules* **2000**, *33*, 9587.
(11) Welch, P.; Muthukumar, M. *Macromolecules* **2000**, *33*, 6159.
(12) Wang, Y.; Kimura, K.; Huang, Q.; Dubin, P. L. *Macromolecules* **1999**, *32*, 7128.
(13) Radeva, T. *Colloids Surf., A* **2002**, *209*, 219−225.
(14) Akinchina, A.; Linse, P. *Macromolecules* **2002**, *35*, 5183−5193.
(15) Chodanowski, P.; Stoll, S. *J. Chem. Phys.* **2001**, *115*, 4951−4960.
(16) Chodanowski, P.; Stoll, S. *Macromolecules* **2001**, *34*, 2320−2328.
(17) Jonsson, M.; Linse, P. *J. Chem. Phys.* **2001**, *115*, 10975−10985.
(18) Messina, R.; Gonzalez-Tovar, E.; Lozada-Cassou, M.; Holm, C. *Europhys. Lett.* **2002**, *60*, 383−389.
(19) Nguyen, T. T.; Grosberg, A. Yu.; Shklovskii, B. I. *J. Chem. Phys.* **2000**, *113*, 1110−1125.
(20) Nguyen, T. T.; Shklovskii, B. I. *Physica A* **2001**, *293*, 324−338. Grosberg, A. Yu.; Nguyen, T. T.; Shklovskii, B. I. *Rev. Mod. Phys.* **2002**, *74*, 329−345.
(21) Joanny, J.-F. *Eur. Phys. J. B* **1999**, *9*, 117−122.
(22) Netz, R. R.; Joanny, J.-F. *Macromolecules* **1999**, *32*, 9026−9040.
(23) Mateescu, E. M.; Jeppesen, C.; Pincus, P. *Europhys. Lett.* **1999**, *46*, 493−498.
(24) Dobrynin, A. V. *J. Chem. Phys.* **2001**, *114*, 8145.
(25) de Vries, R. *J. Chem. Phys.* **2004**, *120*, 3475−3481.
(26) Kolhe, P.; Misra, E.; Kannan, R. M.; Kannan, S.; Lieh-Lai, M. *Int. J. Pharm.* **2003**, *259*, 143−160.
(27) Lyulin, A. V.; Davies, G. R.; Adolf, D. B. *Macromolecules* **2000**, *33*, 3294.
(28) Lyulin, A. V.; Adolf, D. B.; Davies, G. R. *Macromolecules* **2001**, *34*, 8818.
(29) Lyulin, S. V.; Evers, L. J.; van der Schoot, P.; Darinskii, A. A.; Lyulin, A. V.; Michels, M. A. J. *Macromolecules* **2004**, *37*, 3049−3063.
(30) Lee, I.; Athey, B. D.; Wetzel, A. W.; Meixner, W.; Baker, J. R. J. *Macromolecules* **2002**, *35*, 4510. Nisato, G.; Ivkov, R.; Amis, E. J. *Macromolecules* **1999**, *32*, 5895.
(31) van Duijvenbode, R. C.; Borkovec, M.; Koper, G. J. M. *Polymer* **1998**, *39*, 2657.
(32) Lyulin, S. V.; Darinskii, A. A.; Lyulin, A. V.; Michels, M. A. J. *Macromolecules* **2004**, *37*, 4676−4685.
(33) Ryckaert, J.-P.; Bellemans, A. *Chem. Phys. Lett.* **1975**, *30*, 123.
(34) Murat, M.; Grest, G. *Macromolecules* **1996**, *29*, 1278.

MA047403U